Experimental Xanthoma

A Correlative Biochemical, Histologic, Histochemical, and Electron Microscopic Study

Frank Parker, M.D., and George F. Odland, M.D.

IT HAS BEEN KNOWN for many years that experimental xanthomas could be induced in rabbits by means of cholesterol feeding.[1-4] Early studies dealing with histologic and histochemical observations on well-advanced experimental lesions demonstrated the accumulation of lipid containing cells around the small vessels of the dermis.[1,5,6] Other investigators performed limited lipid analyses on plasma and skin at infrequent points in time during cholesterol feeding and related the induced hypercholesterolemia to increased xanthoma cholesterol.[2,4] Recent studies on experimental xanthomas have been primarily biochemical. Utilizing in-vitro techniques, Wilson showed that experimental xanthomas do not synthesize cholesterol, suggesting indirectly that this lipid is primarily derived from the bloodstream.[7] Parker, Peterson, and Odland[8] produced eruptive xanthoma in nontraumatized nuchal skin of rabbits within 4 weeks after initiating cholesterol feeding. The earliest small, papular lesions which consist of a few perivascular foam cells, coalesce in 3–4 months to form planar lesions containing large numbers of macrophages laden with lipids. Comparison of the plasma and skin cholesterol ester fatty acid (CEFA) patterns of these animals at frequent points in time during the evolution of the xanthomas revealed that the normally distinctive CEFA pattern of the skin comes to resemble that of the plasma as the first gross lesions appeared.[8] Thus indirect evidence, based on limited histologic and lipid biochemical studies, has led to the hypothesis that there is an influx of plasma lipid across capillary walls and into the dermis, evoking the accumulation of foam cells which characterize the xanthoma.

Since experimental xanthomas displaying a full spectrum of pathologic alterations can be induced in a relatively brief 4-month span of time, they provide a useful model for comparison with human disease.[8]

From the Department of Medicine, Division of Dermatology, University of Washington School of Medicine, Seattle, Wash.

Supported by Grants AM-08569 and HE-02698 from the U. S. Public Health Service.

Accepted for publication June 11, 1968.

Address for reprint requests: Dr. Parker, Division of Dermatology, Department of Medicine, University of Washington School of Medicine, Seattle, Wash. 98105.

Accordingly, the present investigation correlates analytical and morphologic information derived from modern techniques of lipid biochemistry, electron microscopy, and histochemistry in order to obtain additional evidence regarding the origin of xanthoma lipids.

This study will present ultrastructural evidence that is interpreted as lipid droplets within the dermal capillary walls. It will be emphasized that these fine structural pathologic vascular changes occur simultaneously (4 weeks) with the initial increase in cutaneous lipids and when histochemical observations first reveal lipid droplets in comparable positions in the capillary walls. Ultrastructural study also discloses that subsequent to the initial vascular alterations, foam cells arise from vascular perithelial cells, tissue macrophages, and possibly from wandering lipid-laden cells circulating in the bloodstream.

Materials and Methods

Sixteen mature female albino New Zealand rabbits weighing between 2.5 and 2.9 kg. were used for the several facets of the study. Twelve were fed a 4% cholesterol diet in the manner previously described.[9] The remaining 4 animals served as controls without cholesterol supplements added to the standard diet of Albers Rabbit Breeder Pellets. Both groups of rabbits gained weight in a comparable fashion during the study.

Plasma and nuchal skin specimens were obtained from cholesterol-fed animals at 2-week intervals over a 16-week period. The 4 control rabbits were sampled prior to, and at 8 and 16 weeks after initiating the experiment. The skin biopsies were obtained with the animals under light ether anesthesia after the nuchal area had been shaved with an animal clipper and cleansed with isopropyl alcohol. At the same time, plasma samples for lipid analyses were obtained by cardiac puncture.

Electron and Light Microscopy

At each sampling, two 2-mm. punch biopsies were obtained with a high speed rotary drill from the nuchal area. The biopsies were placed in ice-cold 2% osmic acid buffered with *s*-collidine, pH 7, and fixed for 1½ hr. After fixation, the tissue was dehydrated and embedded in epoxy resin in the manner previously described.[10] Thin sections were cut on a Reichert ultramicrotome, stained with 3% uranyl acetate [11] (10–30 min.) and then lead citrate [12] (3–5 min.) and examined with an RCA-EMU 2C electron microscope. Original magnifications ranged from 1500 to 8000 and further enlargement was achieved photographically.

Sections 1–2 μ in thickness were cut from the same epoxy embedded tissue and stained by the basic fuchsin-methylene blue technique of Huber, Parker, and Odland [13] for examination by light microscopy.

Histochemistry

Thin strips of skin, 0.5–1.0 cm. long, were also taken from the nape of the neck immediately adjacent to the biopsies for electron microscopy. After fixation in 10% formalin for 4 hr., frozen sections were stained for neutral lipid with oil red O,[14] phospholipid with Baker's acid hematin [15] and acid phosphatase.[16]

Chemical Studies

Elliptical pieces of nuchal skin, 4–5 cm. long and 1 cm. wide, enclosing the defects created by the previously mentioned biopsy sites, were removed for lipid analysis. The resulting wound was closed with sterile stainless steel clips. Subsequent sampling did not encroach on previous biopsy sites.

The skin samples were rinsed in cold isotonic saline, and while these were chilling on ice the adherent adipose tissue was carefully dissected away under observation with a dissecting microscope. After blotting dry, the biopsies were weighed, cut into 1-sq. cm. pieces, frozen on dry ice, pulverized in an apparatus similar to that described by Wilhelmji, Kierland, and Owen,[17] and thoroughly homogenized in a tissue grinder.

The lipids of the skin and plasma samples were extracted and washed by the method of Folch, Lees, and Sloane-Stanley,[18] and separated and quantitated by thin-layer chromatography as described by Parker, Rauda, and Morrison.[19] Free and esterified cholesterol,[20] free fatty acids,[21] triglycerides,[22] and phospholipids [23] were subsequently determined.

Observations

Gross Observations

Grossly visible, yellow papules become discernible sparsely scattered over the nape of the neck after 4 weeks of cholesterol feeding.[8] With continued feeding, the papules increased in number and size so that they coalesced by 12 weeks, giving the skin a distinctly yellow and excessively wrinkled appearance. Alopecia was also observed at about this time. No alterations were seen in the nuchal region of control animals.

Plasma and Skin Lipid Alterations

The plasma free and esterified cholesterol increased by 2 weeks and reached a maximum by 4–6 weeks of the experimental period (Text-fig. 1). Plasma phospholipids rose by 4 weeks and remained elevated (Text-fig. 1) while the free fatty acids and triglycerides displayed no significant alteration during cholesterol feeding (Text-fig. 2). Cholesterol esters represented the major lipid accumulating in the blood, with an increase of 20–40 times above the values found in controls. Plasma lipid values for the control animals studied after 8 weeks and at the end of the 16 weeks were not included in the figures since they did not change from the values obtained at the initiation of the study.

In contrast to the plasma lipids which rose in 2 weeks, the increase in skin lipids lagged behind and did not increase significantly until 4 weeks (Text-fig. 3 and 4). In the skin, as well as in the plasma, the major lipids were free and esterified cholesterol (Text-fig. 3). The cutaneous free fatty acids did not change appreciably with time, but after 10 weeks the triglycerides appeared to decrease to approximately one-fourth of the values found in normal skin (Text-fig. 4).

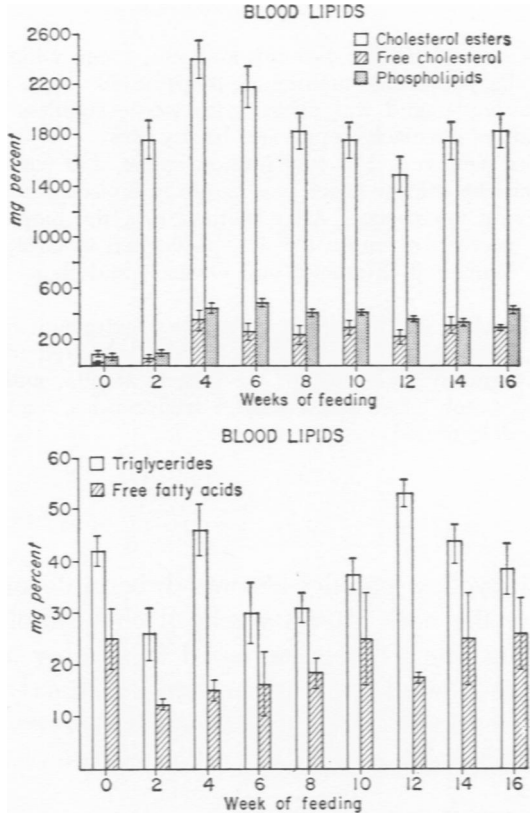

TEXT-FIG. 1 *(top).* Plasma free and esterified cholesterol and phospholipid values are sequentially plotted. The top of each bar represents the mean of 8 rabbits sampled at each interval of time and the horizontal lines above and below the mean delineate one standard deviation. The cholesterol esters and free cholesterol rise rapidly by 2 weeks, peak at 4 weeks, and then plateau. Phospholipids increase by 4 weeks and remain elevated. The values for normal noncholesterol-fed animals is based on the findings in 4 rabbits. The values for these normal animals sampled at 8 and 16 weeks after initiating the experiment are not plotted in this or subsequent tables since these values were comparable to the "0" week values. TEXT-FIG. 2 *(bottom).* Plasma triglyceride and free fatty acids are plotted as in Text-fig. 1. Considerable variation in the mean values for these lipids is seen. There is no significant change from the lipid values of normal, noncholesterol-fed animals.

Light Microscopic Observations

The earliest pathologic alteration observed by light microscopy on the 1-μ plastic-embedded sections was the appearance of vacuoles within cells both in close proximity to and within the walls of blood vessels in the upper and middle dermis (Fig. 1, 2, and 5). This first occurred by 2–4 weeks of feeding. After 4–6 weeks, additional cells, some with cytoplasm sufficiently vacuolated to warrant calling them foam cells, were

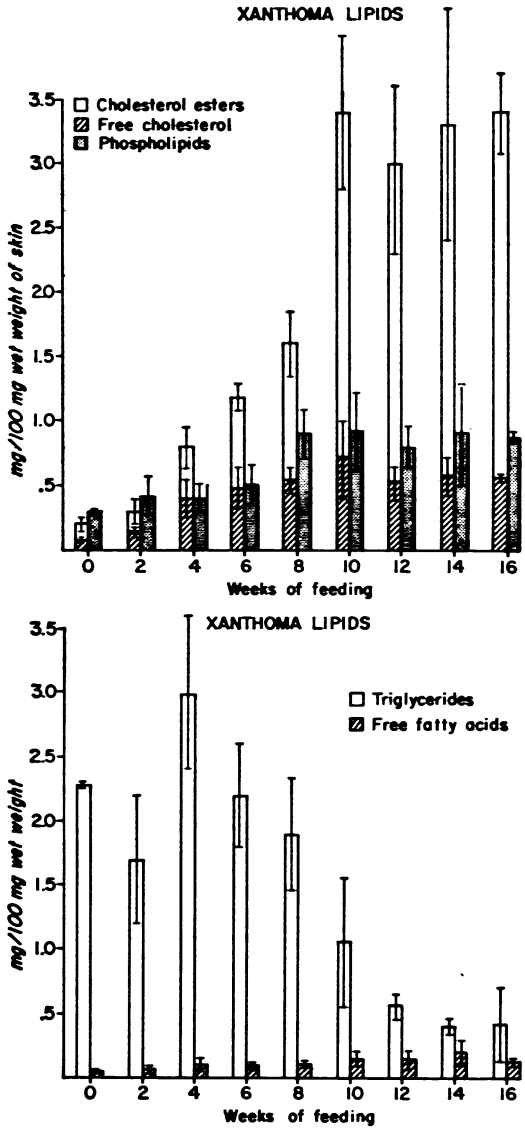

TEXT-FIG. 3 *(top)*. Cutaneous free and esterified cholesterol and phospholipid values sampled at bimonthly intervals after cholesterol feeding are compared to the normal non-cholesterol-fed skin lipids. These 3 lipids increase after 4–6 weeks of cholesterol feeding and then plateau. As in the plasma, the major lipid accumulating is cholesterol ester. The top of each bar represents the mean of 8 rabbits sampled at each interval of time and the horizontal lines above and below the mean delineate one standard deviation. TEXT-FIG. 4. *(bottom)*. Cutaneous triglyceride and free fatty acids are plotted as in Text-fig. 3. No significant change in free fatty acids is found. A significant decrease in triglycerides occurs after the tenth week of feeding, and the decline continues over the next 4 weeks.

observed near the vascular channels (Fig. 2). Still later, by 10–12 weeks, large numbers of foam cells accumulated in the dermis and many of these were remotely situated from blood vessels (Fig. 3). By 16 weeks the upper and middle dermis was almost completely replaced by foam cells (Fig. 4, 5, and 8).

After 10–12 weeks, vacuoles were seen in the smooth-muscle cells of the arrector pili muscles (Fig. 5) as well as in Schwann and perineural cells of the cutaneous nerves (Fig. 6).

Histochemical Studies

Oil red O failed to reveal lipid staining material in the dermis of normal control animals except in the sebaceous glands. However, after 2–4 weeks of cholesterol feeding, lipid droplets were prominent in the vascular walls in locations comparable to those of the vacuolated cells seen in ordinary histologic specimens. In many sections the dermal vessels were brilliantly and precisely outlined by myriads of lipid droplets (Fig. 9 and 10). By 6–8 weeks the cytoplasm of the cells accumulating around vascular channels stained prominently with oil red O. These cells correspond to the foam cells observed with the light microscope. With continued feeding the dermis displayed progressively more intense staining reaction with oil red O, and by 10–12 weeks lipid droplets were seen in arrector pili muscles and dermal nerves.

The foam cells reacted positively with Baker's acid hematin phospholipid stain (Fig. 11). At the same time that the foam cells accumulated significant amounts of neutral fats and phospholipids, the lysosomal enzyme, acid phosphatase, became prominent (Fig. 12).

Electron Microscopic Studies

Normal Skin

In order to provide a basis for comparison with the pathologic events which ensue with cholesterol feeding, the normal appearance of the dermis (Fig. 13) and a small vascular channel (Fig. 14) are shown. Examination of Fig. 13 reveals fibroblasts and a number of blood vessels in collagenous connective tissue. Occasionally macrophages (not illustrated) are encountered.

A normal capillary channel is shown in cross section in Fig. 14. The endothelial cells form a continuous lining by virtue of their close-fitting, interdigitating attachments with one another. Closely applied to the outer surface of the endothelium are elongated pericytes or perithelial cells, whose cytoplasmic process partially invest the capillary.[24] The pericytes are separated from the endothelium by an intercellular space

of 0.2–0.4 μ in width, which largely contains basal lamina enclosing both the endothelial and perithelial cells. The width of this space increases in the pathologic state. The existence of a basal lamina (basement membrane) surrounding the pericyte serves to distinguish this cell from tissue macrophages.

Pathologic Changes with Cholesterol Feeding

Small Vessel Changes. The first pathologic alterations heralding the onset of the xanthomatous lesions occurred at 2–4 weeks in the capillaries of the upper and mid-dermis. One of the most prominent initial changes was the widening of the usually diminutive space between endothelial and perithelial cells (increased to 2–4 μ) as a consequence of the accumulation of variously sized droplets or globules (2000–4000 Å in diameter) near and within the basal lamina of these cells (Fig. 15).

Occasionally droplets were observed midway between the basal lamina and the extracellular space (Fig. 16) and in some cases they even broached the basal lamina and extended out into the extracellular space (Fig. 17).

Concomitant with the appearance of the extracellular droplets, vacuolar spaces were observed in the perithelial cells at 2–4 weeks (Fig. 17 and 18). In some areas the droplets accumulating between the endothelial and perithelial cells appeared to coalesce to form larger globules which deformed and clearly invaginated the pericyte's surface (Fig. 18). Large vacuoles were also seen within the cytoplasm of the pericyte itself. In biopsies taken from more advanced lesions (8 weeks and beyond), extensive vacuolation of pericytes was seen (Fig. 19), giving them an appearance analogous to that of the foam cells of light microscopy (Fig. 1, 2, 5, and 7), as well as those containing lipid droplets stained with oil red O (Fig. 9 and 10).

One additional, infrequently observed alteration of the dermal capillaries which nevertheless was seen often enough to warrant comment, was the presence of vacuolated cells in various positions within and just outside the walls of these vessels (Fig. 20). Such cells, with a distinctive dense-appearing cytoplasm, were occasionally observed within the vascular lumens, between endothelial and perithelial cells and in the extracellular space (Fig. 20).

Extravascular Changes. After 6–8 weeks, and thus slightly later in time than the initial vascular alterations, considerable numbers of both vacuolated and unvacuolated cells seemed to concentrate around the vascular channels (Fig. 21). These appeared to be macrophages containing large numbers of organelles interpreted as lysosomes (Fig. 21,

Inset). It is these cells which reacted positively for acid phosphatase stain (Fig. 12) by light microscopy during the last 8–10 weeks of the experimental period. The macrophages could be distinguished from perithelial cells by their characteristic finger-like microvilli which projected from the cell surface, and because they were not enclosed by a basal lamina (Fig. 22).

With progressive enlargement of the xanthomas, the macrophages increased in number so that by 12–16 weeks they occupied the upper half of the dermis. Little dermal collagen was seen. The macrophages also displayed increasing vacuolation and many contained myelin forms and needle-shaped spaces which we interpreted as cholesterol clefts (Fig. 22). The apparent increase in the number of macrophages and the extent of their cytoplasmic vacuolation seemed to parallel the rise in skin lipids and the increasing intensity of the oil red O and acid hematin phospholipid stains.

The smooth muscle cells of dermal arterioles (Fig. 23) and even of the arrector pili muscles (not pictured) showed vacuolar changes in the late stages of feeding. Some of the vacuolated arteriolar smooth-muscle cells appeared to have more numerous mitochondria than normal (Fig. 23).

Both the Schwann and perineural cells of the cutaneous nerves also contained vacuoles in the later stages of cholesterol feeding (Fig. 21) at a time when oil red O staining revealed lipid droplets in these cells.

Discussion

The relationship of hypercholesteremia to the accumulation of cholesterol in experimental xanthoma has been reported on a number of occasions.[2,4,5] The present study reaffirms this relationship and extends previous observations by sequentially following the plasma and skin lipid alterations induced by cholesterol feeding at frequent points in time over a 4-month period. The rise in plasma lipids, particularly free and esterified cholesterol, precedes the increase of these substances in the skin by 2–4 weeks. This time relationship suggests that xanthoma sterols originate from the plasma. This contention is strengthened by the previous studies of Parker *et al.*,[8] who observed that in rabbits fed cholesterol in a manner similar to that described in the present study, the cholesterol ester fatty acid patterns of skin and plasma come to resemble one another after 1 month. In addition, Wilson demonstrated the failure of xanthomatous tissue to synthesize cholesterol, implying that this lipid is primarily derived from the bloodstream.[7]

Whereas experimental xanthomas accumulate large quantities of cho-

lesterol and phospholipids, this study describes the sequential and progressive decrease in triglyceride after the tenth week of feeding (Text-fig. 4). Thus, in advanced xanthomas, the concentration of triglyceride is only one-fourth of that found in either normal skin or early xanthomas. A similar observation is reported by Johnson and Sanger in avian xanthomas.[25] The reason for this decline in xanthoma triglyceride is not apparent, but it does occur at the time when cholesterol esters reach their maximum (tenth week). Since the quantity of triglyceride is based on the wet weight of the biopsied tissue, the decrease may only be relative to the large quantities of esterified cholesterol accumulating in the skin. It is equally possible that triglyceride is hydrolyzed in the dermis or that it passes into the bloodstream from the tissue.

Earlier observers, concerned with the histology of xanthomas, commented on the presence of lipid within cells near the small vessels of dermis.[1,5,6] Some of these investigators speculated that the lipid was accumulating in the vascular adventitial cells, but they did not define precisely the alterations that might be taking place in and around the vascular wall. It has been possible in this study to show electron microscopic evidence which, when correlated with lipid biochemical and histochemical findings, is interpreted as lipid or lipoprotein particles in transit across the vascular wall. In the electron microscopic studies of Suter and Majno [26] and Schoefl and French,[27] investigating the passage of triglyceride-rich chylomicrons across the dermal capillaries of rats, similar droplets were observed. However, these droplets had a dark appearance in contrast to the apparently empty images described in the present study. The reason for this difference in appearance could be that cholesterol-fed rabbits develop a marked hyperlipemia, but the light-scattering plasma particles contain mainly cholesterol esters which may be more soluble in the fixation procedure utilized for electron microscopy than are triglycerides.[28]

These electron microscopic observations cannot provide definitive evidence as to which direction the lipid particles are moving. From analysis of the sequential quantitative lipid data and cholesterol ester fatty acid patterns,[8] it would appear that the major movement of lipid (cholesterol esters) is from the bloodstream into the skin, but the decrease in skin triglycerides in the course of time also holds forth the possibility of some exchange in the opposite direction. In the present study the endothelial cells appear unaltered. The studies on adult rats [26,27] record the same negative observation. Thus no morphologic explanation can be provided for how the lipid droplets permeate the endothelial cells.

Investigations of vascular permeability utilizing carbon particles as tracers have shown the collection of carbon against the basal lamina in much the same way as the lipid droplets.[29,30] This suggests a filtering action for the basal lamina. However, the droplets can eventually traverse the basal lamina since they may be seen midway between the perivascular space and the vessel wall (Fig. 16), and they can occasionally be seen in the perivascular space itself (Fig. 17).

Once the lipid broaches the basement membrane, it apparently is sequestered by perithelial cells (Fig. 18) and tissue macrophages. Some perithelial cells become extensively vacuolated, and they can justifiably be termed foam cells (Fig. 19). Lipid inclusions within perithelial cells of dermal vessels are also described in newborn rats subjected to physiologic lipemia by Suter and Majno[26] and similar findings have been described in the skin lesions of Fabry's disease, an inborn error of glycolipid metabolism.[31] Thus it may be that the accumulation of lipid substances within the perithelial cell is a more general reaction to various types of physiologic and pathologic stimuli related to alterations of lipid metabolism. The evolution of pericytes into foam cells is of additional interest because these changes are reminiscent of the alterations reported in rabbit coronary and aortic smooth-muscle intimal cells found in early atherosclerotic plaques.[9] It suggests, first of all, that pericytes might be analogous to smooth-muscle cells of large blood vessels and, second, that both cell types react to the accumulation of lipids in the same manner. Indeed, the smooth-muscle cells of dermal arterioles (Fig. 23) and even arrector pili muscles (Fig. 5) show evidence of vacuolation late in the course of feeding, suggesting that this may be universal pathologic response of these cells to tissue hyperlipidemia.

The majority of the foam cells accumulating in the dermis after 4–6 weeks of feeding are not pericytes, however, but rather macrophages. Such cells can be readily distinguished from the perithelial cells with the electron microscope by the submicroscopic anatomic criteria mentioned previously (*see Results*), as well as the presence of large numbers of structures considered to be lysosomes[32] and verified to be such by the acid phosphatase reaction these cells display in frozen sections. Ultrastructurally, the macrophage cytoplasm is dominated by large numbers of vacuoles and occasional needle-shaped spaces thought to represent cholesterol clefts. Some cells also display concentrically arranged lamellas, or so-called myelin forms, which are thought to represent sites of phospholipid deposits.[33,34] Wilson's in-vitro studies on experimental xanthoma metabolism suggest that phospholipid is synthe-

sized in situ rather than originating from the plasma. The finding of myelin forms in the macrophages suggests that these cells are involved in synthesizing such lipid, and the work of Day, Fidge, and Wilkinson [35] on animal macrophages reinforces this assumption.

The origin of the accumulating macrophages is not clearly understood. It is known that the normal dermis contains appreciable numbers of these cells, and it is likely that this source accounts for many of the vacuolated macrophages. In addition, some evidence is presented (Fig. 20) which suggests that vacuolated cells in the circulation may emigrate through the vascular wall. The movement of circulating blood cells across the blood vessel wall has been observed by electron microscopy in a variety of inflammatory conditions,[36] but they have not been previously recorded in experimental xanthomas.

The findings in the present study are summarized in Fig. 24, and they provide both biochemical and, for the first time, ultrastructural evidence to support the theory that blood lipids contribute significantly to xanthoma lipids. In fact, the earliest pathologic alterations seem to be related to the passage of lipid or lipoprotein substances across the vascular wall. Previously published cholesterol ester fatty acid studies showing that experimental xanthoma lipids come to resemble the plasma lipids with cholesterol feeding reinforce the present findings.[8] Under the same experimental conditions employed in these studies, comparable similarities in the cholesterol esters of evolving atheroma of rabbits have also been observed.[8] This finding, taken together with the ultrastructural pathologic similarities occurring in intimal smooth muscle cells of the atherosclerotic plaque and the perithelial cells of the dermal capillaries, suggests that analogous mechanisms may be operating in the formation of xanthomas and atheroma. This leads to the intriguing speculation that certain biochemical and ultrastructural aspects of the initiation and early evolution of experimental xanthomas may significantly reflect similar alterations in the large vessels of the body and thus lead to new insight into the etiology of atherosclerosis.

Summary

The sequential ultrastructural changes occurring in rabbit xanthomas after frequent intervals of cholesterol feeding are described and correlated with quantitative blood and skin lipid analyses, as well as with pertinent histologic and histochemical observations.

Within 2–4 weeks, droplets are seen aggregated within the walls of dermal capillaries. This occurs at a time when blood lipids display their greatest increase, skin lipids initially rise, and oil red O stain on frozen

sections shows lipid droplets in comparable positions. The vacuoles are interpreted as sites of lipid particles in the process of traversing the dermal capillary walls.

At the same time, but more commonly after 4–6 weeks, vacuoles also appear in the perithelial cells and in adjacent accumulating tissue macrophages. Such cells contain lipid-staining droplets on frozen sections, and by this time the skin lipids are increased 3–4 times over controls. With continued feeding, many pericytes become extensively vacuolated and evolve into foam cells. However, most of the developing foam cells are macrophages and their numbers as well as degree of vacuolation appear to increase concomitantly with the quantitative rise in skin lipids.

Certain biochemical and ultrastructural features of evolving experimental xanthoma are compared with the evolution of experimental atheroma, and the possible significance of these findings is discussed.

References

1. SCHAAF, F. On the experimental production of xanthomas in laboratory animals. *J Invest Derm* 1:11–30, 1938.
2. RUSCH, H. P., BAUMANN, C. A., and KLINE, B. E. Production of xanthoma in rabbits. *Arch Path (Chicago)* 28:163–170, 1939.
3. KUNTZ, A., and SULKIN, N. M. Lesions induced in rabbits by cholesterol feeding, with special reference to their origin. *Arch Path (Chicago)* 47: 248–260, 1949.
4. WANG, C., STRAUSS, L., and ADLERSBERG, D. Experimental xanthomatosis in the rabbit. *Arch Path (Chicago)* 63:416–422, 1957.
5. PLEWES, L. W. Nature and origin of the xanthoma cell. *Arch Path (Chicago)* 17:177–186, 1934.
6. WEIDMAN, F. D. Studies in hypercholesterolemia. III. The approach to the pathogenesis of the xanthomas. *Arch Derm (Chicago)* 15:659–668, 1927.
7. WILSON, J. D. Studies on the origin of the lipid components of xanthomata. *Circ Res* 12:472–478, 1963.
8. PARKER, F., PETERSON, N., and ODLAND, G. F. A comparison of cholesterol-ester fatty acid patterns in the blood and in evolving xanthoma and atheroma during cholesterol-feeding of rabbits. *J Invest Derm* 47:253–259, 1966.
9. PARKER, F., and ODLAND, G. F. A correlative histochemical, biochemical and electron microscopic study of experimental atherosclerosis in the rabbit aorta with special reference to the myo-intimal cell. *Amer J Path* 48:197–239, 1966.
10. ODLAND, G. F. "The Fine Structure of Cutaneous Capillaries." In *Advances in Biology of Skin, Blood Vessels and Circulation* (Vol. 2), Montagna, W., and Ellis, R. A. Eds. Pergamon, New York, 1961, pp. 57–70.
11. WATSON, M. L. Staining of tissue sections for electron microscopy with heavy metals. *J Biophys Biochem Cytol* 4:475–478, 1958.
12. REYNOLDS, E. S. The use of lead citrate at high pH as an electron-opaque stain in electron microscopy. *J Cell Biol* 17:208–212, 1963.

13. HUBER, J. D., PARKER, F., and ODLAND, G. F. A basic fuchsin and alkalinized methylene blue rapid stain for epoxy-embedded tissue. *Stain Techn* 43:83–87, 1968.

14. Armed Forces Institute of Pathology. *Manual of Histologic and Special Staining Techniques* (ed. 2). McGraw-Hill, New York, 1960, p. 125.

15. BAKER, J. R. Acid hematin method for choline containing phospholipids. *Quart J Micr Sci* 87:441–445, 1946.

16. BARKA, T., and ANDERSON, R. J. Histochemical methods for acid phosphatase using hexazonium parasanilin as coupler. *J Histochem Cytochem* 10:741–753, 1962.

17. WILHELMJ, C. M., KIERLAND, R. R., and OWEN, C. A. Production of hypersensitivity to skin in animals. *Arch Derm (Chicago)* 86:161–182, 1962.

18. FOLCH, J., LEES, M., and SLOANE STANLEY, G. H. A simple method for the isolation and purification of total lipids from animal tissues. *J Biol Chem* 226:497–509, 1957.

19. PARKER, F., RAUDA, V., and MORRISON, W. H. Quantitative thin-layer chromatography of neutral lipids using semi-specific colorimetric and titrimetric techniques. *J Chromatogr* 34:35–43, 1968.

20. COURCHAINE, A. J., MILLER, W. H., and STEIN, D. B., JR. Rapid semimicro procedure for estimating free and total cholesterol. *Clin Chem* 5:609–614, 1959.

21. DOLE, V. P. A relation between non-esterified fatty acids in plasma and the metabolism of glucose. *J Clin Invest* 35:150–154, 1956.

22. VAN HANDEL, E., ZILVERSMIT, D. B., and BOWMAN, K. Micromethod for the direct determination of serum triglycerides. *J Lab Clin Med* 50:152–157, 1957.

23. BARTLETT, G. R. Phosphorus assay in column chromatography. *J Biol Chem* 234:466–468, 1959.

24. LUFT, J. H. "Fine Structure of the Vascular Wall." In *Evolution of the Atherosclerotic Plaque*, Jones, R. J., Ed. Univ. Chicago Press, Chicago, 1963, pp. 3–14.

25. JOHNSON, R. M., and SANGER, V. L. Lipids in avian xanthomatous lesions. *Amer J Vet Res* 24:1280–1282, 1963.

26. SUTER, E. R., and MAJNO, G. Passage of lipid across vascular endothelium in newborn rats. An electron microscopic study. *J Cell Biol* 27:163–177, 1965.

27. SCHOEFL, G. I., and FRENCH, J. E. "Morphologic Aspects of Vascular Permeability to Fat." In *Fourth European Conference on Microcirculation, Cambridge 1966*, Harders, N., Ed. *Bibl Anat* 9:495–500, 1967.

28. KORN, E. D., and WEISMAN, R. A. I. Loss of lipids during preparation of amoebae for electron microscopy. *Biochim Biophys Acta* 116:309–316, 1966.

29. CASLEY-SMITH, J. R. Endothelial permeability. The passage of particles into and out of diaphragmatic lymphatics. *Quart J Exp Physiol* 49:365–383, 1964.

30. COTRAN, R. S. Delayed and prolonged vascular leakage in inflammation. III. Immediate and delayed vascular reactions in skeletal muscle. *Exp Molec Path* 6:143–155, 1967.

31. SAGEBIEL, R., and PARKER, F. Cutaneous lesions of Fabry's disease: Glycolipid lipidosis. *J Invest Derm* 50:208–213, 1968.

32. WEISSMANN, G. Lysosomes. *New Eng J Med* 273:1084–1090, 1965.

33. CASPER, J., and WOLMAN, M. Demonstration of myelin figures by fluorescence in some pathologic tissues. *Lab Invest* 13:27–31, 1964.

34. STOECKENIUS, W. An electron microscope study of myelin figures. *J Biophys Biochem Cytol* 5:491–500, 1959.

35. DAY, A. J., FIDGE, N. H., and WILKINSON, G. N. Effect of cholesterol in suspension on the incorporation of phosphate into phospholipid by macrophages in vitro. *J Lipid Res* 7:132–140, 1966.

36. MARCHESI, V. T., and FLOREY, H. W. Electron micrographic observations on the emigration of leukocytes. *Quart J Exp Physiol* 45:343–348, 1960.

The authors gratefully acknowledge the invaluable contributions of Mr. James D. Huber, who prepared the tissues for electron and light microscopy, and Miss Donna Gorder, who carried out the lipid analyses. Thanks are gratefully given to Mr. Johsel Namkung, of the Department of Pathology, for the preparation of the color plate, and to Mr. Charles A. Oclassen and Westwood Pharmaceuticals for providing the funds to publish the colored plate.

The authors also wish to thank their colleagues in the Department of Biological Structure, who generously permitted the use of their electron microscopic facilities.

Legends for Figures

Figures 13–23 are electron micrographs.

Fig. 1. Animal fed 2 weeks. Small dermal vessel with vacuoles *(V)* within perivascular cell *(P)* and in one foam cell *(FC)* at some distance from the vessel. × 500.

Fig. 2. Vascular channel in mid-dermis from animal fed 4 weeks. There are vacuoles in the perithelial cells *(P)* as well as in a number of foam cells *(FC)* nearby, but they are clearly separate from the vascular wall. Myelinated nerve fiber *(N)*. × 400.

Fig. 3. Area of mid-dermis from animal fed 10 weeks. A vascular channel *(BV)*, cut longitudinally, courses through center of the field. A large number of foam cells are situated near the vessel and in more remote positions as well. × 400.

Fig. 4. By 16 weeks of cholesterol feeding, the upper and middle dermis is almost completely replaced by foam cells. Some foam cells have cholesterol clefts *(CC)*. Two vascular channels *(BV)* are visible close to the epidermis *(EP)*. Vacuolation of the vascular pericytes is seen. × 350.

Fig. 5. Arrector pili muscle with some vacuoles in the smooth-muscle cells courses diagonally through the dermis of animal fed 14 weeks. Numerous foam cells replace most of the collagen normally seen, and 2 vascular channels *(BV)* show extensive vacuolation of the perithelial cells. × 350.

Fig. 6. Vacuolation of Schwann cells of a dermal nerve from a rabbit fed 10 weeks. Dense oval structures are myelin surrounding axon cylinders. A few foam cells are adjacent to the nerve. × 900.

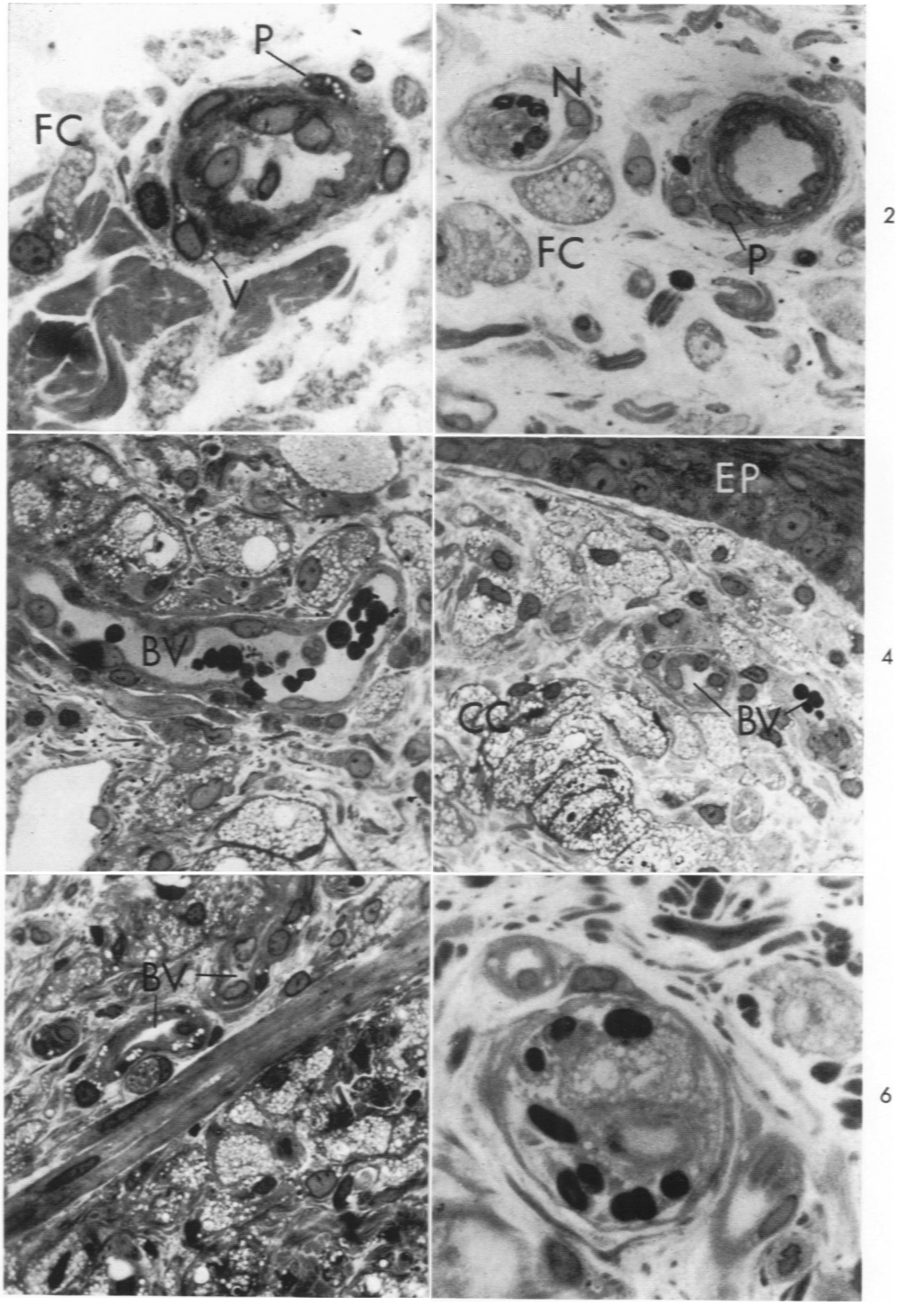
1
P
FC
V
2
N
FC
P
3
BV
4
EP
CC
BV
5
BV
6

Fig. 7. Specimen from a rabbit fed cholesterol for 4 weeks. Note 3 vascular channels *(BV)* coursing through the center of the picture. Vacuoles are seen in pericytes *(P)* and a few adjacent foam cells *(FC)*. Red blood cells and polymorphonuclear leukocytes are in lumens of two vessels. Collagen *(C)* appears blue. Section (1 μ), embedded in plastic, is stained with basic fuchsin and alkalinized methylene blue as described by Huber *et al.*[13] × 400.

Fig. 8. Specimen from a rabbit fed cholesterol 16 weeks. Epidermis *(EP)* is at top. Dermis is dominated by large numbers of closely packed, highly vacuolated foam cells. Two vascular channels *(BV)* are observed. Collagen appears blue. Plastic embedment, 1-μ section, Huber stain. × 300.

Fig. 9. Dermis from animal fed 4 weeks. Two vascular channels *(BV)* are clearly outlined by numerous lipid droplets. Adjacent cells *(FC)* contain lipid droplets as well. These cells are comparable to those observed in Fig. 7. Frozen section, oil red O stain. × 200.

Fig. 10. Section from rabbit fed 4 weeks. A blood vessel is sectioned longitudinally and the walls contain numerous lipid droplets. Adjacent perivascular cells *(FC)* also contain lipid. Frozen section, oil red O stain. × 800.

Fig. 11. Section from rabbit fed 12 weeks. Epidermis appears at upper left. Dermis contains many foam cells which react positively (blue color), confirming the lipid analytical findings that significant quantities of phospholipid reside in the foam cells or macrophages. Frozen section, Baker's acid hematin phospholipid (choline) stain. × 600.

Fig. 12. Frozen section from animal fed 10 weeks. Epidermis is at upper left, and numerous foam cells in the dermis stain prominently for acid phosphatase. × 400.

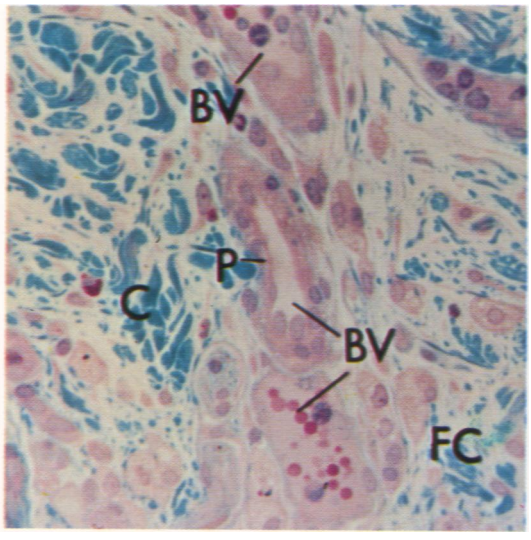

7

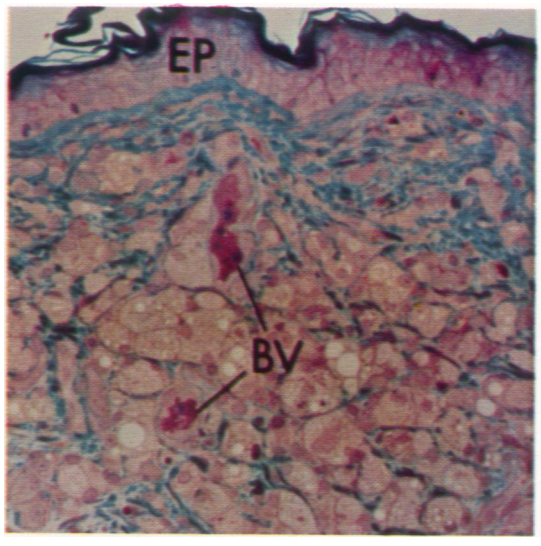

8

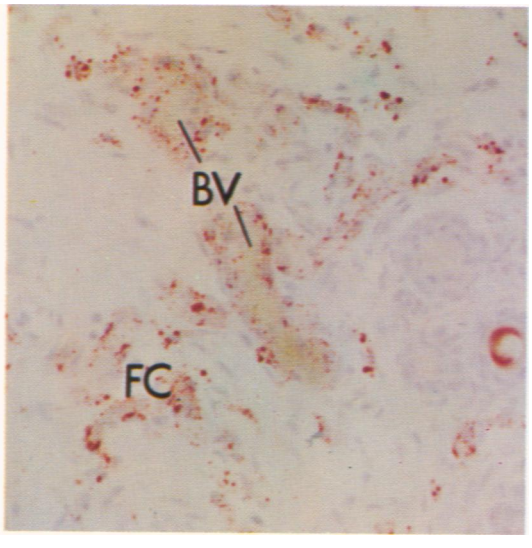

9

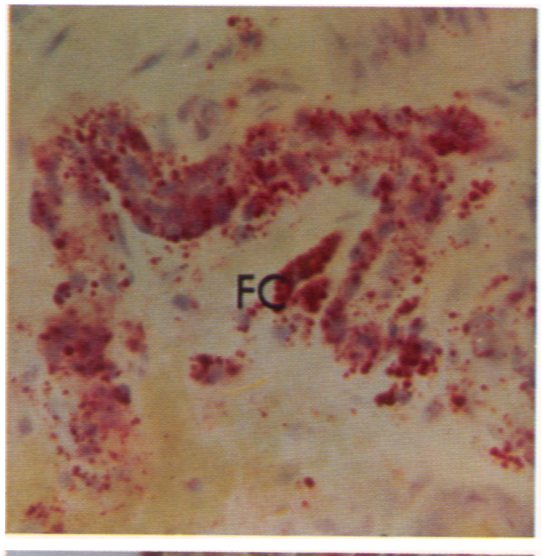

10

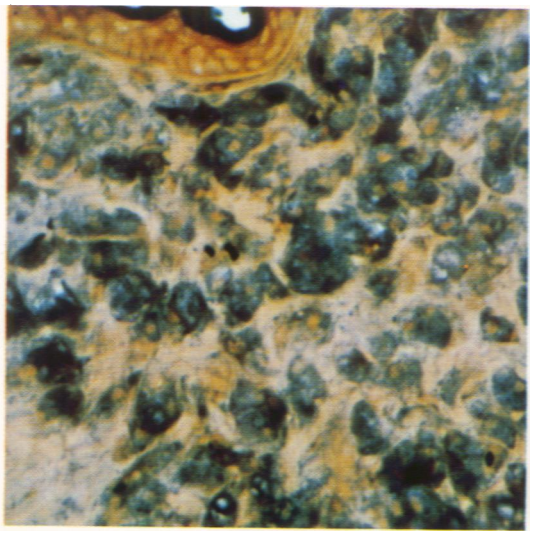

11

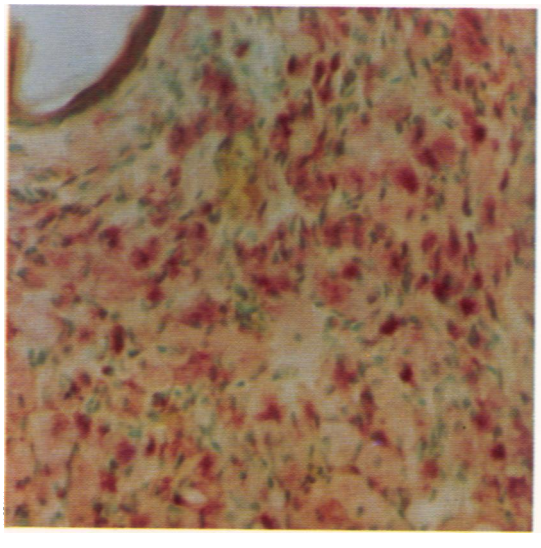

12

Fig. 13. Small portion of dermis from a normal control animal after 8 weeks on a regular diet of rabbit feed is shown for comparison with appearance of dermis from an advanced xanthoma (Fig. 21). Three vascular channels *(BV)* appear in cross section, with a number of fibroblasts *(F)* and bundles of collagen *(C)* interspersed between them. The vascular lumens are collapsed and appear only as narrow slits. Prominent nuclei of both endothelial cells *(E)* and pericytes *(P)* are seen. × 2750.

Fig. 14. Normal dermal vascular channel cut in cross section displays profiles of portions of red blood cells *(R)* in the lumen. Endothelial cells *(E)* form a continuous lining and are partially invested by pericytes *(P)* which appear as elongated cells, thicker in the center where the nucleus resides and extending thin cytoplasmic tongues out circularly around the endothelium. The pericytes are separated from the endothelial cells by an intercellular space of small but variable dimensions (0.2–0.4 μ). Other than this close apposition to the endothelium, the pericytes have no distinguishing characteristics although their cytoplasm does contain fine filaments. Both endothelial and perithelial cells are enclosed by a basal lamina *(B)*. × 10,150.

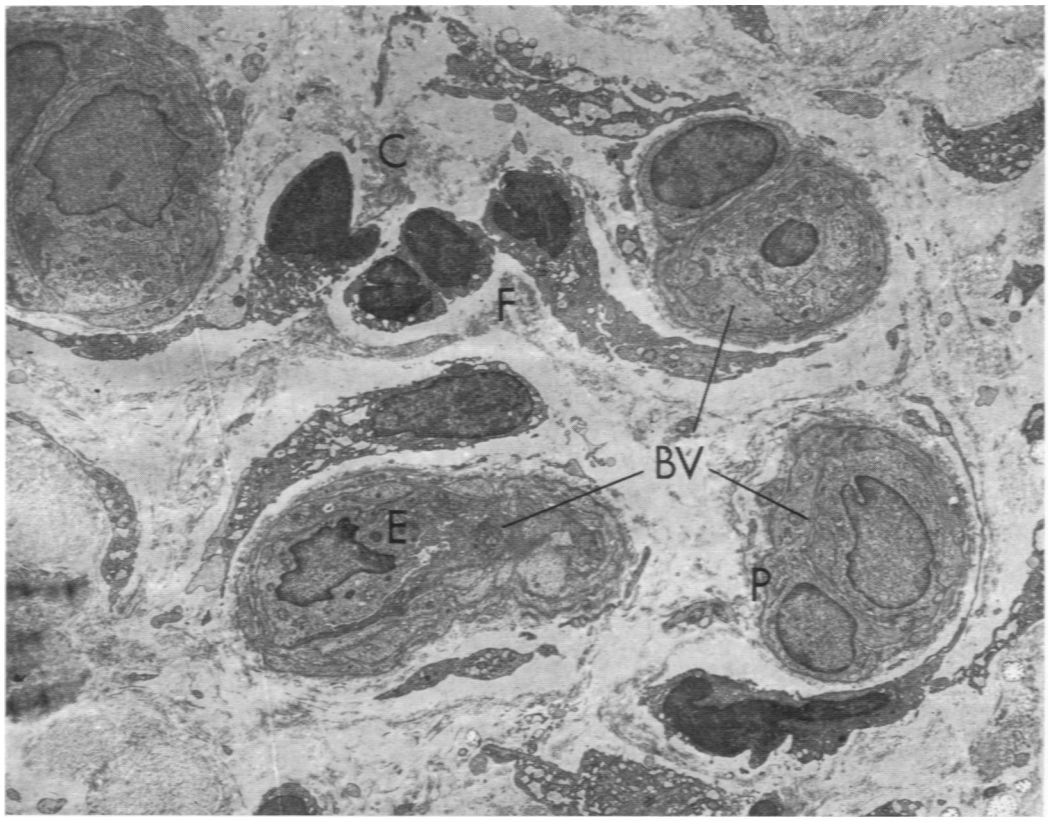

13

14

Fig. 15. Dermal vascular channel from animal fed 4 weeks, showing widening of subendothelial space in a number of places around the vessel, owing to the collection of droplets *(D)* against the basal lamina *(B)* and pericytes *(P)*. The lumen *(L)* of the vessel is collapsed and appears as a narrow slit. A portion of a macrophage *(M)* is in close proximity to the capillary; its cytoplasm contains a few vacuolar spaces. × 10,000.

Fig. 16. Animal fed 6 weeks. An extensive accumulation of droplets *(D)* is seen within the blood vessel wall. A few larger droplets appear to be midway between the basal lamina and the extracellular space *(ES)*. The profile of a portion of a red blood cell *(R)* is seen in the vessel lumen. Endothelium, *E*. × 14,875.

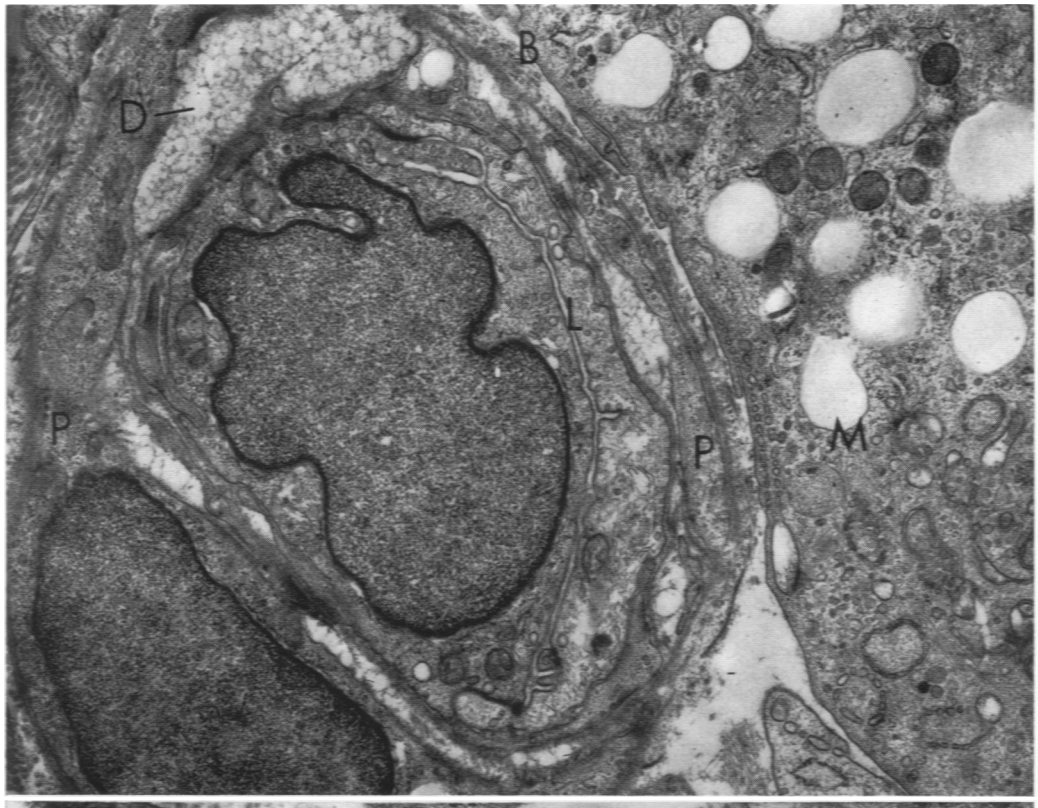

15

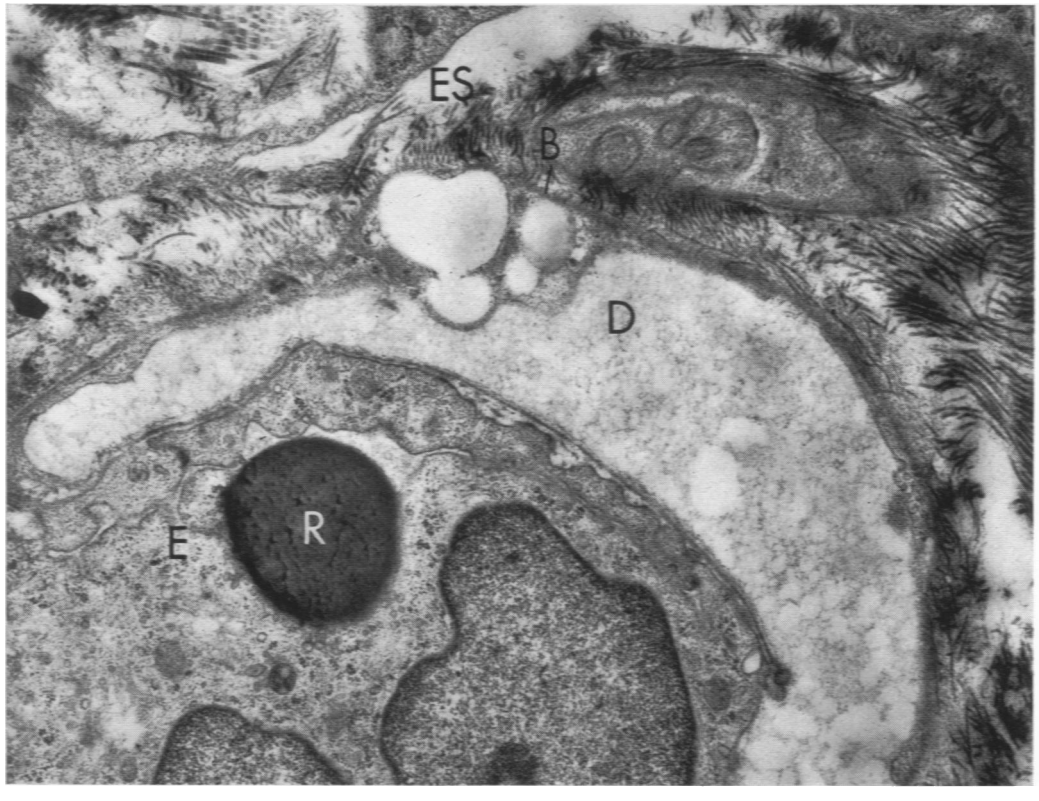

16

Fig. 17. Extensive pathologic alterations appear in this dermal capillary taken from a rabbit fed 10 weeks. Although endothelial cells *(E)* are intact, outlining a patent vascular lumen *(L)*, large numbers of droplets *(D)* are seen between endothelial and perithelial cells *(P)* and extend out into the extracellular space *(ES)*. Numerous breaks in the basal lamina *(B)* are seen. Pericytes contain a number of cytoplasmic vacuoles *(V)*. Collagen, *C*. × 10,000.

Fig. 18. Small portion of a dermal capillary from an animal fed 6 weeks. Small droplets *(D)* are aggregated between the endothelium *(E)* and a pericyte *(P)*. In some areas the small droplets appear to coalesce into larger droplets which deform and invaginate the subendothelial surface of the pericyte. Large vacuoles *(V)*, some containing dense material, are also apparent in the perithelial cytoplasm. Lumen, *L*. × 14,875.

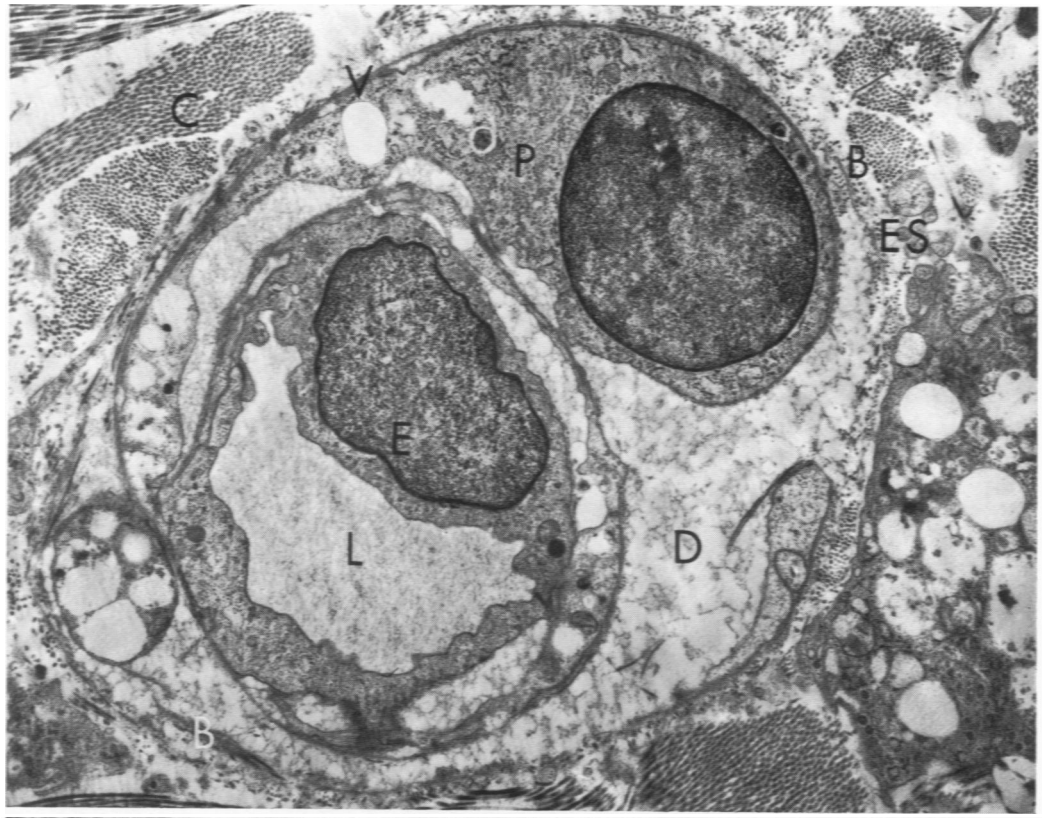

17

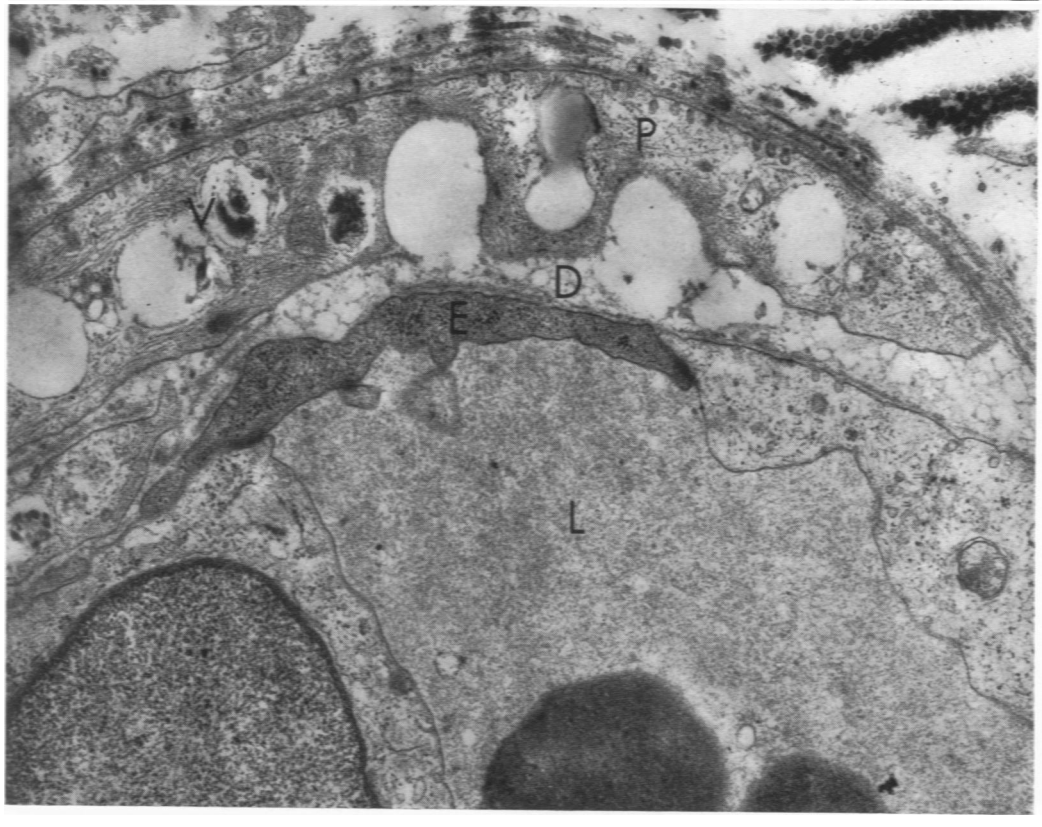

18

Fig. 19. Portion of a foam cell *(FC)* is in close proximity to a dermal capillary obtained from a rabbit fed cholesterol for 10 weeks. The foam cell is identified as a pericyte since a basal lamina *(B)* clearly circumscribes it, in contrast to the lack of such a structure in tissue macrophages shown in Fig. 21 and 22. Two other pericytes *(P)* are also vacuolated, and small extracellular droplets are clearly seen, aggregated against the perithelial cells and the capillary basal lamina. Vascular lumen, *L.* × 6500.

Fig. 20. Animal fed 6 weeks. Portions of two cells with distinctive dense-appearing cytoplasm, inclusions, and numerous vacuoles. The profile of one cell is within the capillary wall, lodged between the endothelium *(E)* and a pericyte *(P)*, while the second is in the extracellular perivascular space *(ES)*. Lumen, *L.* × 10,000.

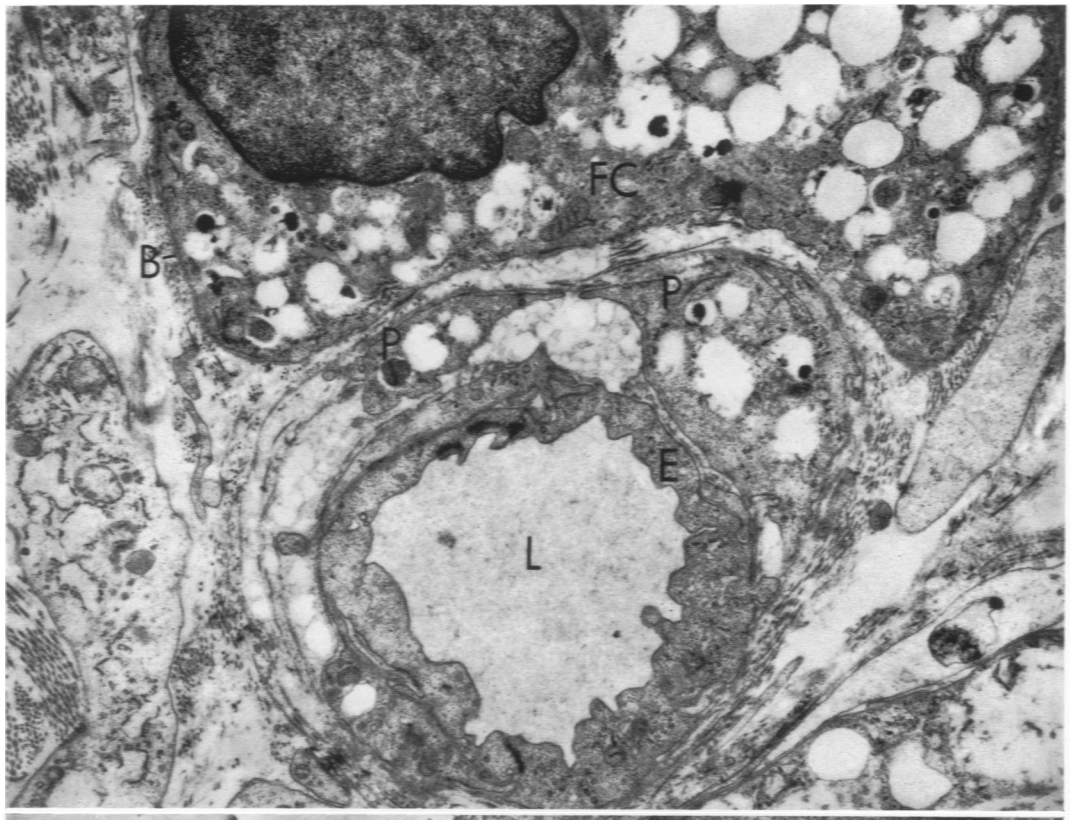

19

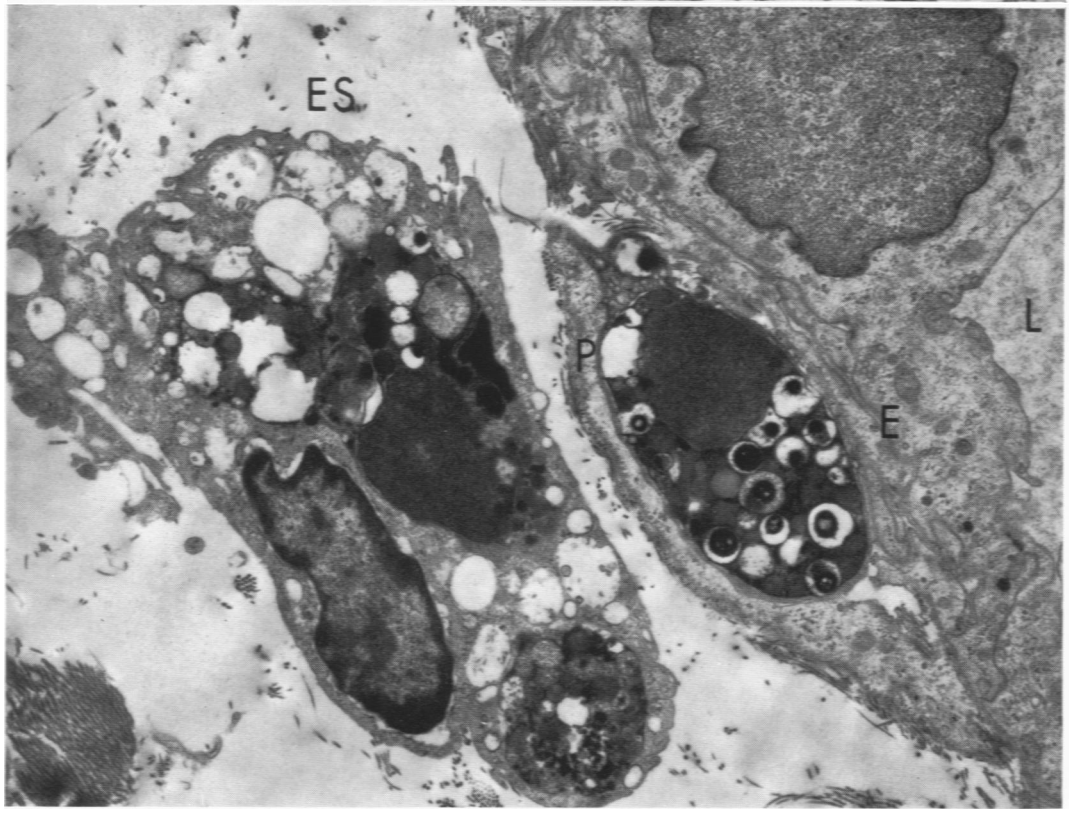

20

Fig. 21. Portion of mid-dermis from animal fed 16 weeks. This picture corresponds to the light micrographs, Fig. 4 and 8. A number of vacuolated macrophage foam cells *(M)* dominate the dermal region near a vascular channel *(BV)* and two nerve fibers *(N)*. Both Schwann *(S)* and perineural cells *(PN)* of the nerve fibers contain vacuoles. × 2750. **Inset.** Animal fed 12 weeks. Portion of the cytoplasm of a macrophage foam cell, showing a vacuole *(V)* and lysosomal structures *(LY)*. × 14,875.

Fig. 22. Portion of a macrophage foam cell from a far advanced xanthoma (animal fed 14 weeks). Cytoplasm contains a number of vacuoles *(V)*, some of which appear empty while others contain myelin forms *(MY)*. A cholesterol cleft is also apparent *(CC)*. No basal lamina is seen surrounding this cell, and characteristic microvilli *(MV)* on the surface distinguish this cell from a pericyte. × 10,000.

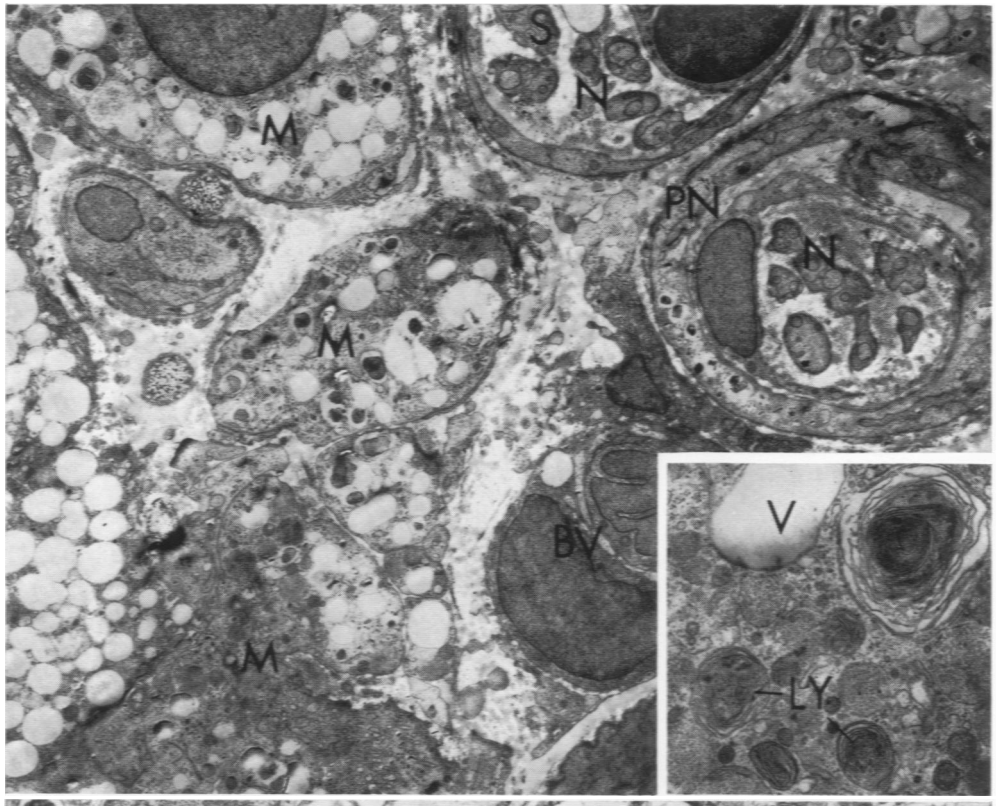

21

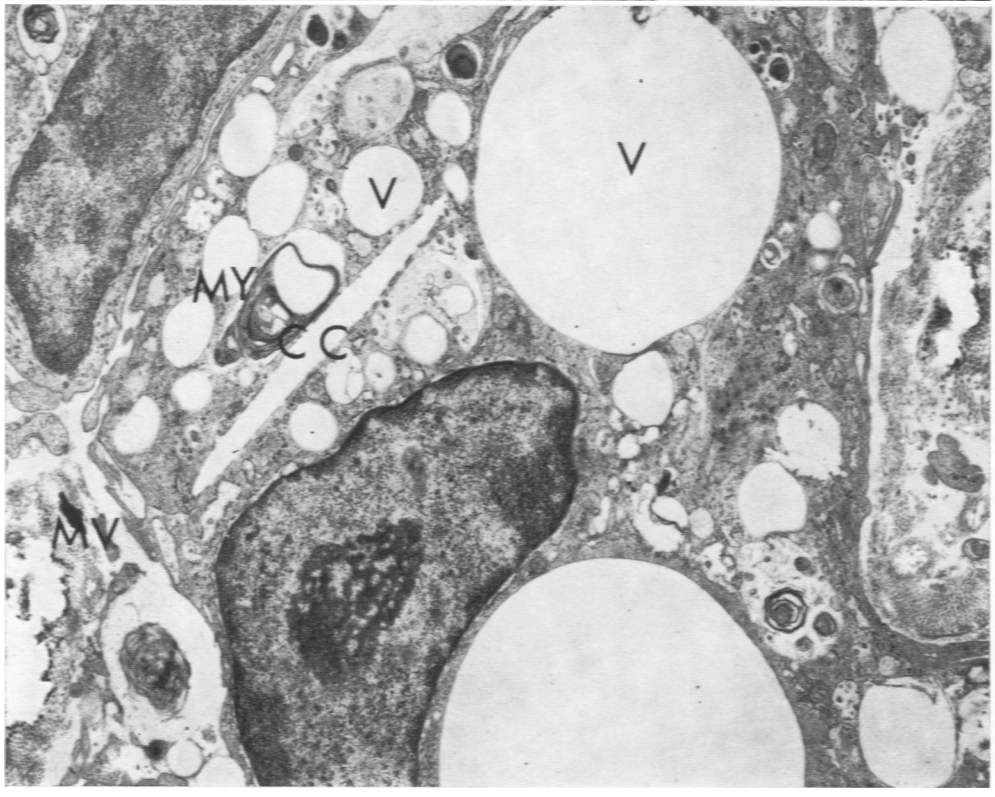

22

Fig. 23. Smooth-muscle cell *(SM)* of a dermal arteriole contains numerous vacuoles in the cytoplasm. The presence of dense bodies and myofilaments identifies this as a smooth-muscle cell.[9] Mitochondria aggregated around the vacuoles appear to be more numerous than are normally present. Endothelium *(E)* appears normal. Lumen, *L.* × 6500.

Fig. 24. Schematic summary of results of the present investigation. General changes in blood lipids *(solid line)* and skin lipids *(dotted line)* during cholesterol feeding are compared and a brief recapitulation of the salient ultrastructural pathologic events is superimposed.

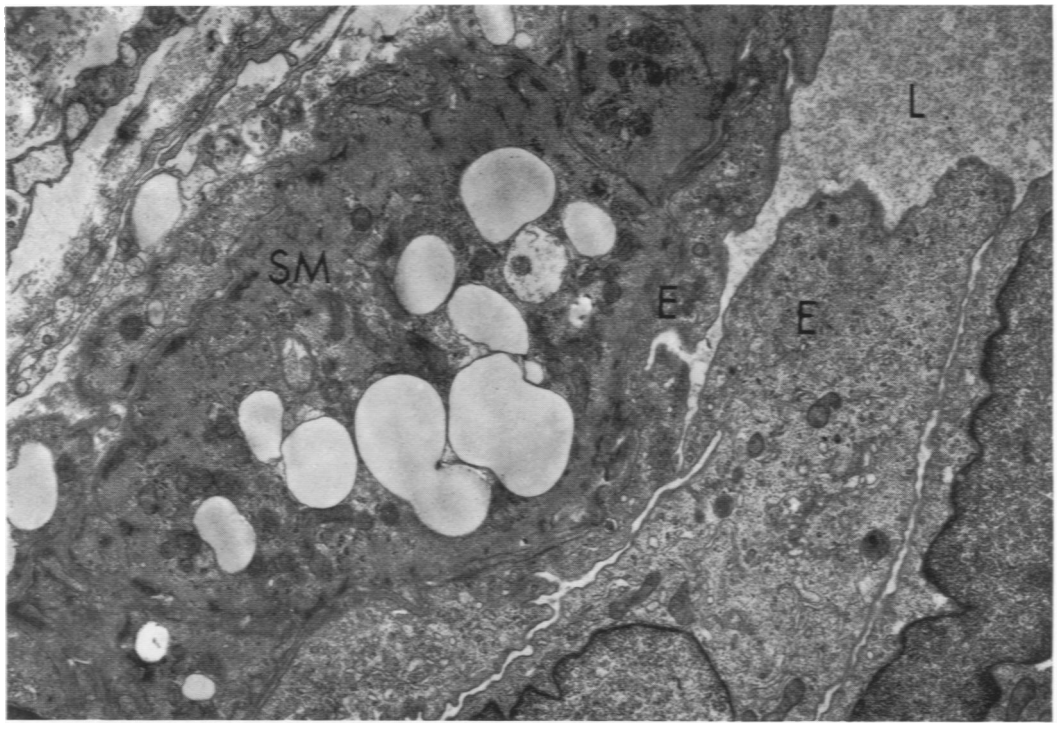
L
SM
E
E

23

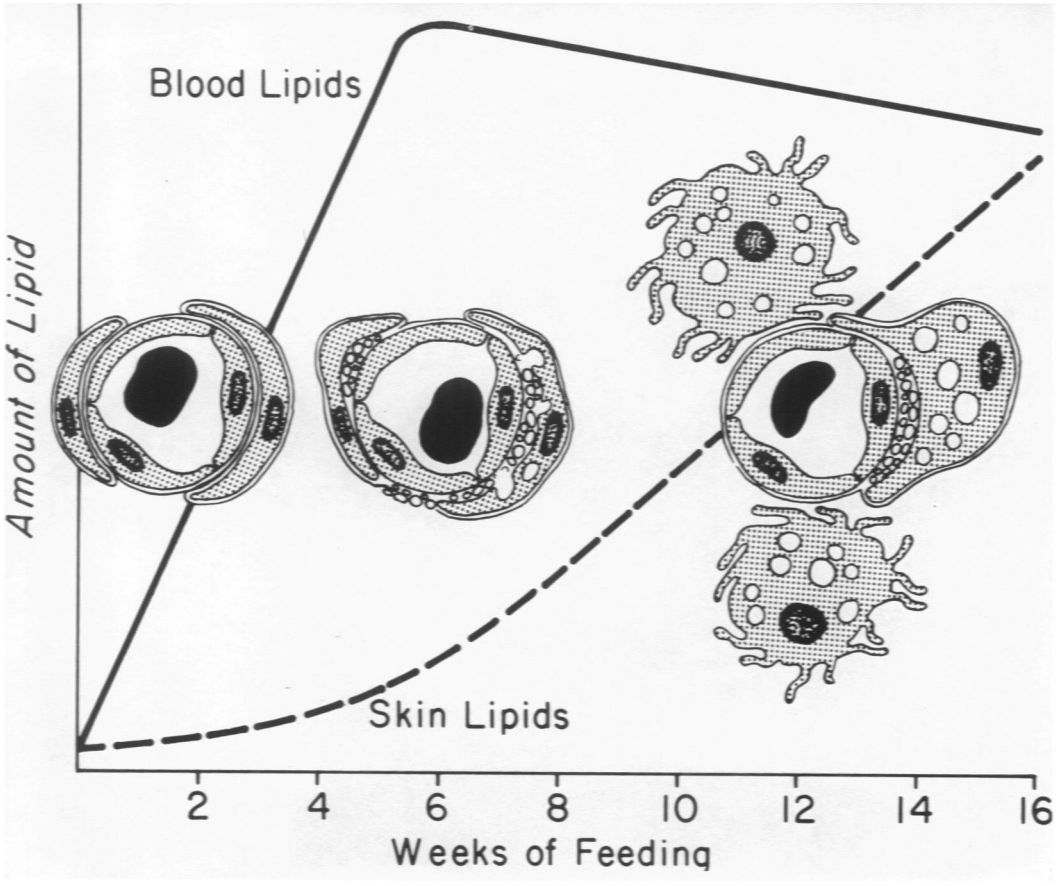
Blood Lipids
Amount of Lipid
Skin Lipids
2
4
6
8
10
12
14
16
Weeks of Feeding

24